

TABLE I
CIRCUIT PARAMETER SENSITIVITIES FOR TYPICAL DATA

	$ S_{11} $	$\angle S_{11}$	$ S_{12} $	$\angle S_{12}$	$ S_{21} $	$\angle S_{21}$	$ S_{22} $	$\angle S_{22}$
C_{gd}	-0.49	0.03	0.99	0.08	-0.01	0.08	-0.38	0.01
C_{ds}	1.14	-0.13	-2.38	-0.63	-1.77	-1.30	2.36	3.35
C_{gs}	-0.09	1.36	-0.36	-0.02	-0.26	-0.04	0.14	-0.003
R_i	-97.80	-0.96	-0.06	7.77	-0.27	16.55	0.21	0.31
g_m	-0.69	0.03	-0.01	0.05	0.99	0.13	-0.38	0.01
τ	679.20	-26.08	6.78	-53.28	8.70	-565.07	-9.25	-10.39
R_{ds}	-0.03	-0.02	0.04	-0.22	0.04	-0.46	2.16	-0.03
ξ	-97.90	0.40	-0.43	7.75	-0.53	16.50	0.35	0.30

III. RESULTS AND DISCUSSION

The sensitivities corresponding to a typical set of data are shown in Table I. For the devices tested at the WAMI Laboratory, University of South Florida, Tampa, for instance, workers have long recognized the input resistance R_i as a notoriously unstable parameter when determined numerically from S -parameter measurements. Our analysis pinpoints the difficulty. Table I shows a 97.80 sensitivity of R_i with respect to $|S_{11}|$ (for our device). Subject to the limitations and approximations described above, this would predict that a 1% error in the parameter $|S_{11}|$ causes an error of 98% in the element R_i . Since our equipment (a Hewlett-Packard HP8510B Network Analyzer) typically exhibits errors in the range of 3%–5% in this parameter under the test conditions,¹ R_i clearly cannot be determined accurately from S -parameter data.

The least reliably determined circuit element is the time-delay τ , for which our calculations show enormous sensitivities to both $|S_{11}|$ and $\angle S_{21}$. The parameter $|S_{11}|$, as stated above, is subject to 3%–5% measurement errors. The angle $\angle S_{21}$ for this data is approximately 167°, and phase measurement errors typically run around 5°,¹ or around 3%. (Indeed, phase errors are usually absolute, not relative quantities; one may wish to omit the normalizations in the phase factors for the phase condition numbers (3).) Thus, any determination of τ is completely swamped by its uncertainty. The difficulty in establishing accurate values for the time delay from S -parameter measurements is well known, and frequently τ is simply omitted from the model.

Condition-number analysis highlights the numerically unstable elements in the model, with respect to a specific experimental determination (i.e., via S -parameters). It identifies which particular S -parameters limit the accuracy of the results, and it tells us how accurately these must be measured in order to derive reliable circuit element values. These sensitivities are due to ill conditioning of the mathematical equations relating the circuit elements to the S -parameters. They are inherent in the model-plus-extraction procedure itself and are, therefore, algorithm independent.

However, they do not imply that the model is unverifiable. Alternative experimental procedures could conceivably finesse these high sensitivities. For instance, we found that the sensitivities of this model's elements with respect to the Y -parameters were fairly benign (thus, the villain in the piece was the ill conditioning of the Y -parameters with respect to the S -parameters). If Y -parameters could be measured directly, one could model nonlinear transistors much more accurately.

¹ Hewlett-Packard Company, *System Manual HP8510B Network Analyzer*, P/N 08510-90074, Santa Rosa, CA, July 1987.

REFERENCES

- [1] G. W. Stewart, *Introduction to Matrix Computations*. New York: Academic, 1973.
- [2] N. J. Higham, "A survey of componentwise perturbation theory in numerical linear algebra," in *Proc. Symp. Appl. Math. Amer. Math. Soc.*, pp. 1943–1993.
- [3] A. D. Snider, L. P. Dunleavy, F. D. King, and D. P. Levinson, "Two more condition numbers for $\mathbf{A}\mathbf{x} = \mathbf{b}$," *Numerical Linear Algebra Applicat.*, submitted for publication.
- [4] M. Berroth and R. Bosch, "Broad-band determination of the FET small-signal equivalent circuit," *IEEE Trans. Microwave Theory Tech.*, vol. 38, pp. 891–895, July 1990.
- [5] S. F. Adam, *Microwave Theory and Applications*. Englewood Cliffs, NJ: Prentice-Hall, 1969.

New Tunable Phase Shifters Using Perturbed Dielectric Image Lines

Ming-yi Li and Kai Chang

Abstract—This paper presents new tunable phase shifters using perturbed dielectric image lines (DIL's). The propagation constant in the DIL was perturbed by a movable metal reflector plate installed in parallel with the ground plane of the DIL. The phase shift was thus controlled and adjusted by varying the perturbation spacing between the DIL and movable reflector plate at a given operating frequency. A rigorous hybrid-mode analysis was used for calculating the dispersion of propagation constants in the perturbed DIL, and then for designing tunable phase shifters. Ka-band tunable phase shifters have been designed, fabricated, and tested. Measurement results agree well with theoretical predictions. The device is especially useful for millimeter-wave applications where traditional phase shifters are lossy.

Index Terms—Dielectric image lines, millimeter waves, tunable phase shifters.

I. INTRODUCTION

Dielectric image lines (DIL's) have reduced losses compared to microstrip lines at millimeter-wave frequencies since most of the signal travels in the low-loss dielectric region [1]. This structure was recently proposed for feeding the aperture-coupled microstrip-patch antenna arrays [2]–[4], and overcomes the high conduction loss problem of microstrip lines at millimeter-wave frequencies. A phase shifter is one of the important control circuits used extensively at microwave and millimeter-wave frequencies. Traditional phase shifters use solid-state or ferrite devices. In this paper, new tunable phase shifters using DIL's are described. The DIL can be transformed to rectangular waveguide or microstrip line using transitions.

In a DIL, the electromagnetic (EM) signal travels mainly inside the dielectric and can be perturbed in several ways. The changing of propagation constants of an EM field in the DIL can be applied

Manuscript received July 17, 1997; revised May 5, 1998. This work was supported by the NASA Lewis Research Center and the Texas Higher Education Coordinating Board's Advanced Technology Program.

The authors are with the Department of Electrical Engineering, Texas A&M University, College Station, TX 77843-3128 USA.

Publisher Item Identifier S 0018-9480(98)06150-X.

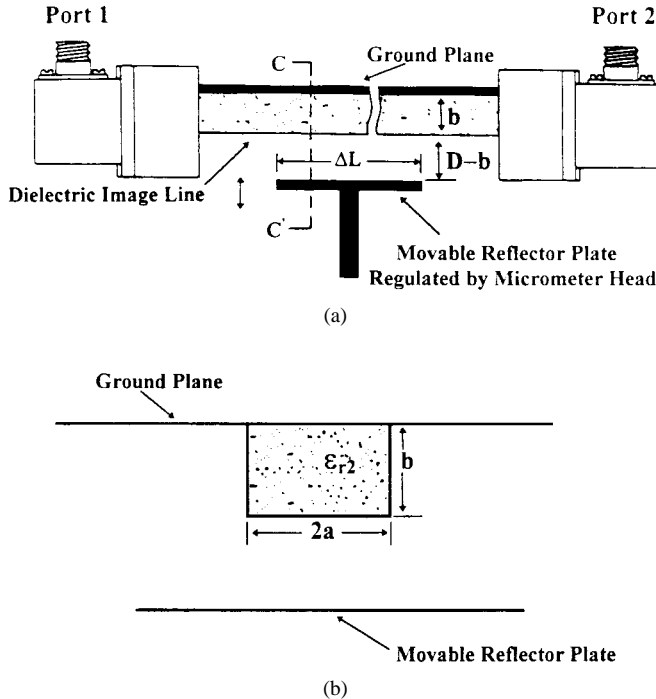


Fig. 1. (a) Structure of a tunable phase shifter using a perturbed DIL. (b) Cross-sectional view at $C - C'$.

to vary the phase difference. This paper reports the perturbation of propagation constant in the DIL by a movable metal reflector plate installed in parallel with the ground plane of the DIL. The phase shift was controlled and adjusted by changing the perturbation spacing between the DIL and movable reflector plate at an operating frequency. The movement can be controlled mechanically or electromechanically using a motor or piezoelectric materials. The tunable range of phase shifters principally relies on the dispersion property of EM-wave propagation constants in DIL's. The structure is simple, low-cost, easy to be fabricated, stable, and reliable.

The DIL was generally analyzed using the effective dielectric constant (EDC) method [1], [5], [6]. It is an approximate calculation and cannot be used to analyze the perturbed DIL structure with a movable reflector plate (DILWRP). In this paper, a rigorous hybrid-mode analysis was used for calculating the dispersion of EM-field propagation constants in the perturbed DIL structures, and then for designing tunable phase shifters. Ka-band tunable phase shifters using a DILWRP have been designed, fabricated, and tested. It had good impedance match, wide frequency operation, and large tunable ranges. Experimental results agree very well with theoretical predictions.

II. CONFIGURATIONS

Fig. 1(a) shows the structure of a tunable phase shifter using a perturbed DIL, and Fig. 1(b) shows the cross-sectional view at $C - C'$. A movable metal reflector plate is installed in parallel with the ground plane of the DIL to form a DILWRP structure. The perturbation spacing between the DIL and movable reflector plate is controlled and precisely adjusted using a micrometer head. For testing purposes, the signal is coupled to the DIL from the waveguide through transitions. Proper design of DIL dimensions allows single-mode propagation for a considerable range of frequency [1]. The phase shift between ports 2 and 1 of the structure without a movable reflector plate depends on the length of the DIL and the propagation

constant in the DIL

$$\Phi_{21} = L \cdot \beta_g + \Phi_0 \quad (1)$$

where L is the length of the DIL, $\beta_g = 2\pi/\lambda_g$ is the propagation constant in the DIL, and Φ_0 is the phase due to transitions and connections, which can be calibrated out using proper calibration techniques. The propagation constant β_g in the DIL is changed when a movable metal reflector plate is installed and the perturbation spacing is varied. This results in a tunable phase shift

$$\Delta\Phi_{21} = \Delta L \cdot \Delta\beta_g \quad (2)$$

where ΔL is the perturbation length in the DIL, and $\Delta\beta_g$ is the perturbed propagation constant in DIL. The tunable range of the phase shifter is controlled by ΔL and $\Delta\beta_g$, and may be raised by making ΔL larger and increasing the perturbation of propagation constants $\Delta\beta_g$. The structure of tunable phase shifters given above is simple, low-cost, easy to fabricate, and reliable. The phase shifts can be easily controlled.

III. RIGOROUS HYBRID-MODE ANALYSIS AND THEORETICAL RESULTS

Accurate computation of propagation constants and λ_g in the perturbed DIL with a movable reflector plate is required for theoretically predicting the phase shifts. A rigorous hybrid-mode analysis [7] was used in this paper for calculating the dispersion of propagation constants in the DILWRP and then for designing tunable phase shifters.

Fig. 2 is the configuration of a DIL of width $2a$, height b , and relative dielectric constant ϵ_{r2} . A movable perfect electric reflector plate is placed at a distance D ($z = -D$) in parallel with the ground plane ($z = 0$). The perturbation of the reflector plate to EM field properties in the DILWRP can be adjusted by changing the distance D . DILWRP structures will become DIL when D increases to infinity. The cross-section region with DIL under the ground plane is subdivided into four subregions I-IV. A complete set of field solutions is derived for each subarea. The dependence of field components on x can be assumed to be an exponential function as $\exp(\pm j\beta_g x)$. β_g is the phase propagation constant and is the same in all these four subregions. y - and z -dependencies of fields in regions I-IV are formulated using eigenfunctions, so that boundary conditions are fulfilled on defined boundaries. All modes are classified as TM and TE with respect to the z -direction. Fields in every subregion can be expressed in terms of scalar potential functions for TM and TE to z -modes. Boundary conditions are enforced independently. Finally, a complex matrix equation is derived. All matrix elements are functions of frequency f , perturbation spacing D , image line sizes, dielectric constant ϵ_{r2} , and propagation constant β_g . All data except β_g in these matrix elements can be calculated when f , D , image line sizes, and ϵ_{r2} are given. Propagation constants β_g in the DILWRP are computed by determining the zeros of the determinant of the whole complex matrix equation. The effect of different perturbation spacing D on propagation constants β_g is then accurately computed.

For a given operating frequency and DILWRP structure characteristics, the determinant of the complex matrix is computed and examined for its zero crossing for β_g in the range between β_0 and $\beta_0\sqrt{\epsilon_{r2}}$. Propagation constants β_g are then determined. The complex double precision is used in calculating the determinant. A sufficient number of imaginary roots has to be solved and used, and the right imaginary roots have to be chosen in order to get convergent and accurate numerical results. The correct way to choose real and imaginary roots has been studied and found in this paper. Accurate results and fast

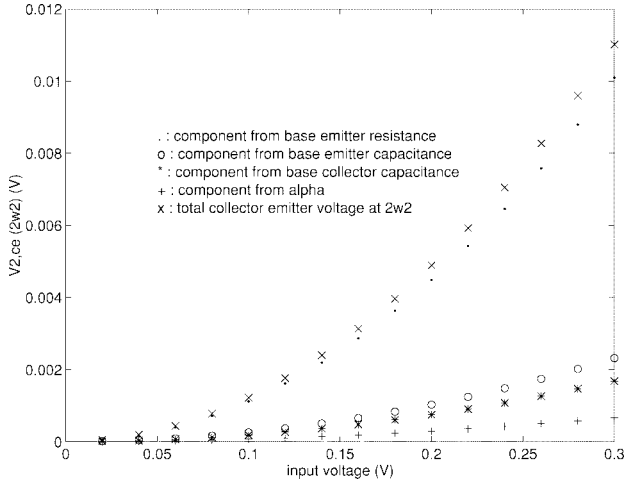
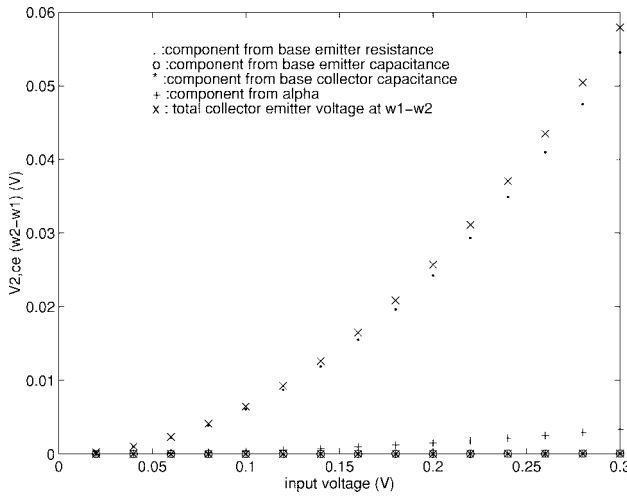
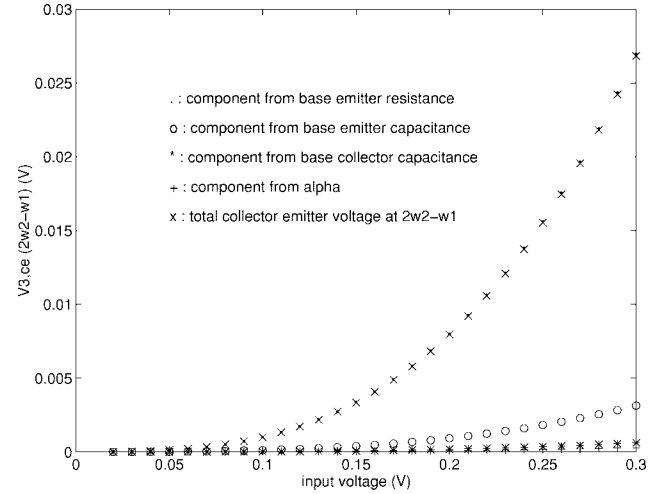


Fig. 2. DILWRP.

Fig. 3. Calculated propagation constants β_g for the Ka-band DILWRP. Image line sizes: 1.27 mm \times 2.54 mm, $\epsilon_{r2} = 10.5$, $D = 10.0$ mm.

convergence can be achieved using only five TE modes and five TM modes, which include four real modes and one imaginary mode.

Fig. 3 shows calculated results β_g for Ka-band DILWRP structures. The relative dielectric constant of the DIL in all cases was 10.5. Image line sizes were 1.27 mm \times 2.54 mm. The perturbation distance D was chosen as 10.0 mm. Five TE modes and five TM modes were used in all computation with a calculation accuracy better than 1%. Results of propagation constants β_g were found to increase when the operating frequency increased. Propagation constants β_g in the DILWRP have been seen to be different when the perturbation distance D changes. Fig. 4 gives numerical results of β_g in the Ka-band DILWRP for different distance D at 29.0 and 35.0 GHz. β_g was found to increase 11.5% at 29.0 GHz and 5.71% at 35.0 GHz when distance D decreased from 10.0 to 1.3 mm. The EDC method is an approximate method and can be used only for an image line without reflector plate, which is the special case of the DILWRP with an infinitive perturbation spacing D . The H-guide is another special case of the DILWRP when D is equal to the thickness b of the DIL. Calculated results using the EDC method [1], [5], [6] and H-guide theory [1] are also given in Fig. 4 for comparison. It can be seen that theory agrees well with the results calculated using the EDC method and H-guide theory for these two special cases.

Fig. 4. Computed propagation constants β_g for the Ka-band DILWRP with different distance D at 29.0 and 35.0 GHz. Image line sizes: 1.27 mm \times 2.54 mm, $\epsilon_{r2} = 10.5$. —●—: 29.0 GHz, —■—: 35.0 GHz, hybrid mode analysis: \times EDC method, $*$: H-guide theory.

IV. EXPERIMENTAL RESULTS

Operating frequency range, propagation constants β_g in the DIL, perturbation spacing D , and the effect of different D on β_g are several key parameters for designing tunable phase shifters using the DILWRP. They determine the tunable range of a phase shifter. Ideally, the DIL should be kept as large as possible at a given operating frequency range, especially for millimeter-wave applications, in order to ease fabrication problems and lessen the effects of size variations on the guide wavelength and scan angle. At the same time, single-mode operation must be maintained in the propagation of the signal in the DIL in order to achieve accurate phase shifts. The unit ratio of the DIL size of $a/b = 1$ provides the maximum bandwidth [1]. For good field containment and single-mode operation, the following formula can be used to select unit aspect ratio a/λ_0 for DIL structures:

$$\frac{a}{\lambda_0} \approx \frac{0.32}{\sqrt{\epsilon_{r2} - 1}}. \quad (3)$$

The relative dielectric constant ϵ_{r2} of the DIL should be chosen not too small in order to get enough dispersion in DIL's, and then to realize large phase-shift ranges. $\epsilon_{r2} = 10.5$ is a good choice for the Ka-band frequency range from our experience.

The rigorous hybrid mode analysis was used to design the DILWRP. RT-Duroid material of relative dielectric constant $\epsilon_{r2} = 10.5$ was used to make the DIL. The Ka-band DIL had $2a = 3.00$ mm and $b = 1.27$ mm. A diameter of 6.0 mm of the movable reflector disk was installed in parallel with the ground plane of the DIL to form a DILWRP. The perturbation length ΔL was then equal to 6.0 mm. A micrometer head was used to precisely control the perturbation distance to an accuracy of 1 mil.

The Ka-band tunable phase shifter showed good input impedance match, low insertion loss, wide frequency operation, and large tuning phase-shift range. Fig. 5 gives satisfied measurement results of the insertion loss in an Ka-band tunable phase shifter. Less than 2.0-dB insertion loss was realized, which included losses in the DIL with a length of 110 mm and in two waveguide-to-DIL transitions. The movable reflector plate did not deteriorate the performance of insertion loss and return loss even when the perturbation spacing ($D - b$) was close to 1 mm. Fig. 6 shows experimental and theoretical results of phase shifts for different perturbation spacing ($D - b$) at 35 GHz. Tuning ranges approximately 90° were reached for the perturbation length $\Delta L = 6.0$ mm when the perturbation spacing

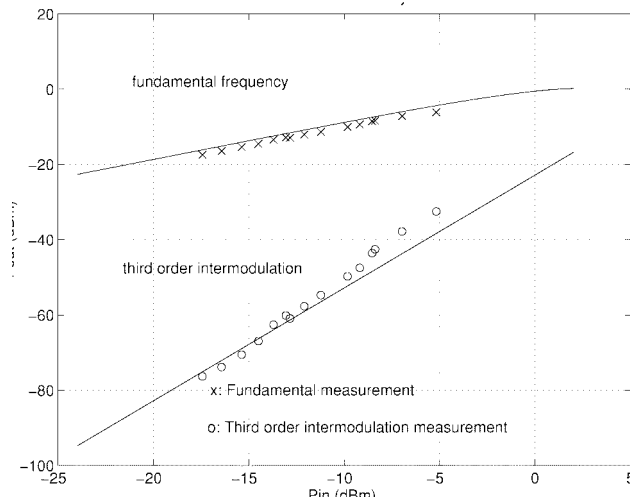


Fig. 5. Experimental insertion loss results of the *Ka*-band tunable phase shifter, which includes all losses in the DIL and in two waveguide-to-DIL transitions.

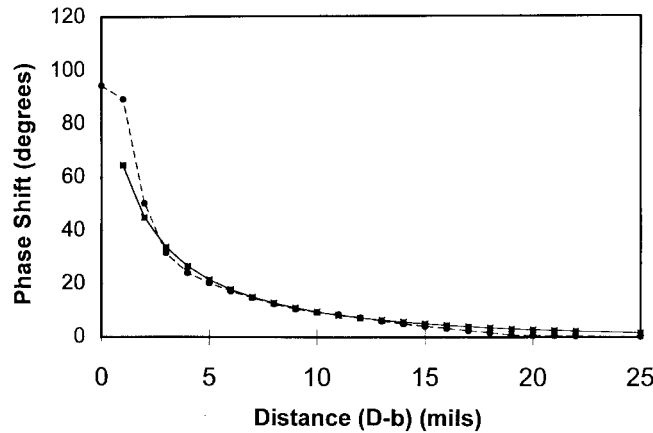


Fig. 6. Phase shifts for different perturbation spacing ($D - b$) at 35 GHz.
—■—: theoretical, —●—: experimental.

($D - b$) changed from 25 to 1 mil. The tuning range of phase shifts can be increased further using longer ΔL . Measurement data agreed well with theory prediction in all operating frequencies.

V. CONCLUSIONS

New tunable phase shifters using perturbed DIL's have been presented in this paper. The propagation constant in the DIL was perturbed by a movable metal reflector plate installed in parallel with the ground plane of the DIL. A micrometer head was used to precisely control the perturbation spacing. The phase shift was adjusted by varying the perturbation spacing at a given operating frequency. A rigorous hybrid-mode analysis was used for calculating the dispersion of propagation constants in the DIL, and then for designing tunable phase shifters. The structure is simple, low-cost, easy to fabricate, stable, and reliable.

Ka-band tunable phase shifters using the DILWRP have been designed, fabricated, and tested. Tunable phase shifters showed good impedance match, low insertion loss, wide frequency operation, and large tuning phase-shift range. Less than 2.0-dB insertion loss was realized, which included all losses in the DIL and in two waveguide-to-DIL transitions. The movable reflector plate did not deteriorate the

performance of insertion loss and return loss of the phase shifter even when the perturbation spacing ($D - b$) was close to 1 mm. Tuning ranges approximately 90° were accomplished for the perturbation length $\Delta L = 6.0$ mm, and could be increased further using longer ΔL . Measurement data agreed well with theoretical predictions.

ACKNOWLEDGMENT

The authors would like to thank Dr. S. Kanamaluru and Dr. J. A. Navarro for their helpful suggestions and useful discussion.

REFERENCES

- [1] P. Bhartia and I. J. Bahl, *Millimeter Wave Engineering and Applications*. New York: Wiley, 1984.
- [2] M. Y. Li, S. Kanamaluru, and K. Chang, "Aperture coupled beam steering microstrip antenna array fed by dielectric image line," *Electron. Lett.*, vol. 30, pp. 1105–1106, July 1994.
- [3] S. Kanamaluru, M. Y. Li, and K. Chang, "Design of aperture coupled microstrip antenna array fed by dielectric image line," *Electron. Lett.*, vol. 31, pp. 843–845, May 1995.
- [4] —, "Analysis and design of aperture coupled microstrip patch antennas and arrays fed by dielectric image line," *IEEE Trans. Antennas Propagat.*, vol. 44, pp. 964–974, July 1996.
- [5] R. M. Knox and P. P. Toulios, "Integrated circuits for the millimeter through optical frequency range," in *Proc. Symp. Submillimeter Waves*, New York, NY, Mar. 1970, pp. 497–516.
- [6] T. Itoh and B. Adelseck, "Trapped image guide for millimeter wave circuits," *IEEE Trans. Microwave Theory Tech.*, vol. MTT-28, pp. 1433–1436, Dec. 1980.
- [7] K. Solbach and I. Wolff, "The electromagnetic fields and the phase constants of dielectric image lines," *IEEE Trans. Microwave Theory Tech.*, vol. MTT-26, pp. 266–274, Apr. 1978.